

BOILING MORPHOLOGY AND HEAT REMOVAL OF IMPINGING COOLANT DROPLETS

A. S. Moita*, A. L. N. Moreira

Technical University of Lisbon – Instituto Superior Técnico

Av. Rovisco Pais, 1049-001 Lisbon, Portugal

*Corresponding author: anamaita@dem.ist.utl.pt

ABSTRACT

The present paper concerns the study of the boiling mechanisms, at the solid-liquid interface, of single droplets impacting onto heated targets and their relation with thermal induced atomization mechanisms, within the various boiling regimes. Droplet impact is recorded with two synchronized high-speed cameras, positioned to obtain both side and bottom views of the same impinging droplet. The heat transfer measurements complement the quantitative information required to characterize the cooling performance of the system. There is a time gap between the beginning of the boiling process and the triggering of the thermal induced atomization, which depends on the liquid and on the surface properties. The liquid droplets with smaller surface tension and smaller latent heat of evaporation are more likely to undergo a faster boiling process, promoting the disruption of the lamella and generation of dry regions. The thermal induced atomization further decreases the contact area and residence time of the lamella, thus degrading their cooling performance. This degradation on the cooling performance due to the dynamic behaviour of the droplet, which is altered during the boiling process can be balanced by altering the targets. These differences are less evident as one approaches the CHF condition and may be compensated by changing the surface.

INTRODUCTION

The development of thermal management strategies for electronic parts, alternative to conventional cooling systems is an interdisciplinary topic of interest involving diverse research fields, from Materials Science to Fluid Dynamics [1]. Among the existing strategies, direct liquid cooling systems such as spray cooling and particularly those based on phase change, are promising technologies capable of removing high heat fluxes, (e.g. [2]). However, the thermal and fluid dynamic mechanisms involved are still poorly understood and further investigation is required to adequate the design parameters (e.g. [3]). On the other hand, recent applications suggest combining the use of sparse sprays or droplet impingement systems with textured surfaces to improve the cooling performance. For instance, Amon et al. [4] report higher heat fluxes using textured surfaces in their embedded droplet impingement system for integrated cooling of electronics, which is under development. Similar trend was observed by Hsieh and Yao [5] using cone sprays at very low flow rates impinging onto textured surfaces. Using a similar argument, Kim [6] supports that a more efficient fluid management can be achieved by combining the use of a sparse spray with textured surfaces. Given this scenario, the fundamental knowledge based on single droplet impacts becomes an important tool in the prompt development of these systems, capable of providing guidelines in terms of the most adequate design parameters to consider.

In this context, in previous work (e.g. Moreira et al. [7], Moita and Moreira [8]), fluid dynamics and secondary atomization mechanisms were associated with the heat transfer mechanisms, based on the combined analysis of the temporal evolution of secondary droplets characteristics

with temperature profiles, measured at the impact of single droplets onto heated surfaces. This procedure allowed to identify the most important periods of droplet dynamic behaviour (e.g. triggering of the secondary atomization and most intense boiling periods) and to relate them to the most relevant periods of the cooling performance. Early results presented in [7,8] suggest that the contact period and contact area of the lamella are strongly dependent on the liquid properties but are significantly altered by the roughness parameters, which must be carefully chosen in order to ensure a better performance of the system, when using textured surfaces with well defined topographic characteristics. Therefore it is important to optimize this contact area and period to promote an effective heat removal by phase change, both in droplet impingement but also in spray cooling systems, (e.g. as in Panão and Moreira [9] who showed the potentialities of using a Direct Contact Intermittent Cooling System, which was further confirmed in practical systems with dynamic boundary conditions, such as those considered in Moita et al. [10]). Nevertheless, in order to determine the surface characteristics optimizing the contact period and contact area of the impinging droplet, it is necessary to have an accurate temporal and spatial description of the boiling mechanism. In line with this, the work presented here deepens the study of the boiling morphology, performing a detailed analysis of the boiling structures, based on image analysis of both side and bottom views of droplets impacting onto heated surfaces, to provide a more accurate description of the processes involved in the thermal induced atomization and their relation with the boiling and heat transfer mechanisms. Several theoretical studies on the boiling mechanisms are reported in the literature (e.g. Buyevich and Webbon [11]), but the description of these structures within the spreading droplet and at the liquid-surface interface is still sparsely

investigated, exception made, for instance to Chaves et al. [12] and to Kandlikar and Steinke [13]. Therefore, the analysis reported here concerns the qualitative and quantitative description of the boiling mechanisms, in time and space, and their relation with the triggering of the secondary atomization mechanisms, thus allowing a more accurate characterization of the boiling regimes. The heat transfer measurements, following the work, for instance, of Chen and Hsu [14] and Pasandideh-Fard et al. [15], complement the quantitative information required to characterize the cooling performance of the system.

EXPERIMENTAL ARRANGEMENT

The experiments reported here encompass the use of different liquids impacting onto heated targets at variable conditions, within a wide range of Weber and Reynolds numbers ($65 < We < 1314$; $170 < Re < 8680$). Surface temperatures were varied from room temperature up to 350°C , thus covering the entire range of boiling regimes, from the nucleate up to the film regime ($T_w > \text{Leidenfrost}$), for the pairs liquid/surface in study. Given the context of an application to electronic systems, the experiments encompass the use of droplets of different liquids, including a dielectric fluid, the methoxy-nonafluorobutane, $\text{C}_4\text{F}_9\text{OCH}_3$ (HFE7100). Table 1 summarizes the thermo-physical properties of the working fluids.

Liquid	HFE7100	Water
Properties		
<i>Surface Tension</i> [Nm ⁻¹] $\times 10^3$ (20°C)	13.6	73.75
<i>Density</i> [kgm ⁻³] (20°C)	1430	998
<i>Kinematic viscosity</i> [m ² s ⁻¹] $\times 10^6$ (20°C)	3.8	1.0
<i>Specific heat</i> [KJKg ⁻¹ K] (25°C)	1.18	4.18
<i>Latent heat of vaporization</i> [KJKg ⁻¹] (25°C)	122.6	2272

Table 1: Thermo-physical properties of the working fluids.

Several target plates were used, both opaque (metallic) and transparent, in order to obtain complementary information on the boiling structures and on their relation with the thermal induced atomization mechanisms. Metallic targets are accommodated on a copper base inside which a 264W cartridge heater was inserted. The temperature of the targets is monitored by thermocouples type K and controlled by a PMA KS20-I temperature controller. One of the thermocouples is a fast response “Medtherm” eroding-K-type which is embedded at the centre of the impact region of the target plates. The signal of the thermocouples is sampled with a National Instruments DAQ board plus a BNC2120 and amplified with a gain of 300 before processing.

Transparent surfaces, used to provide optical access to the interface liquid-solid are smooth glass targets heated by Joule effect from the back side with a transparent film of Indium Oxide, In_2O_3 . Deposition of the film is made by radio frequency (rf) plasma enhanced reactive thermal evaporation (rf-PERTE) at low substrate temperature ($< 100^\circ\text{C}$). Details of the method and of the resulting relevant film properties are reported by Carvalho et al. [16]. A similar method has been used to study heat transfer in two phase micro channel flows by Silvério and Moreira [17]. The authors detail the advantages, from the heat transfer point of view, of using pure In_2O_3 instead of doping it with Ti, SnO_2 or Ag, as reported by other authors. Temperature of these targets is monitored by contact type K thermocouples positioned over the glass side.

The targets were characterized by the equilibrium contact angle, θ and by the surface topography. The topography is quantified by the roughness amplitude (mean roughness, R_a , determined according to standard BS 1134 and mean peak-to-valley roughness, R_z , calculated according to standard DIN4768) and by the fundamental wavelength, λ_R when the surface is regular (for the textured surfaces). The complete characterization of all the target plates and their wetting behaviour with the various liquids used in the experiments (performed at room temperature) is depicted in Moita and Moreira [18], so that only a summary of the main characteristics of the targets used in this study, in terms of material topography and *wettability* with water is presented in Table 2. Complete wetting ($\theta \approx 0^\circ$) is observed at room temperature for all surfaces, when wetted by the HFE7100.

Surface		R_a [$\mu\text{m} \pm 10\%$]	R_z [μm]	λ_R [μm]	θ [$^\circ$]
Glass	Random profile	~ 0	~ 0	-	13.2
	Regular profile (textured surfaces)	17.1	81.5	210	-
Aluminum	Random profile	1.0	13.76	-	75.3
	Regular profile (textured surfaces)	16.7	92.3	430	-
Stainless steel	Random profile	0.311	2.32	-	-
	Regular profile (textured surfaces)	42.0	175.3	530	-

Table 2: Main characteristics of the target plates.

The temporal and spatial characterization of droplets impact is made with two high-speed cameras (a Kodak Motion Corder Analyser, Series SR 512x420pixels, Model PS-120, with maximum frame rate of 10kfps and a Phantom v4.2 from Vision Research Inc., with 512x512pixels@2100fps, with maximum frame rate of 90kfps) which are positioned to obtain both side and bottom views of the droplet. Both cameras are synchronized and triggered to start recording at the passage of the droplet, thus allowing the simultaneous characterization of side views (e.g. to describe secondary atomization) and bottom views (e.g. to study the boiling morphology on the liquid-surface interface) of the same impinging droplet. This information, complemented with the temperature measurements upon droplet impact, allow to analyze the whole fluid dynamics and heat transfer processes leading to thermal induced atomization during droplet/wall interactions.

RESULTS AND DISCUSSION

The present study considers the analysis of the boiling mechanisms and their relation with the thermal induced atomization. In this sense, temporal and spatial characterization of the impact is made with two synchronized high-speed cameras positioned to obtain both side and bottom views of the same droplet. The former allows the characterization of the mechanisms of disintegration of the lamella upon the surface and of the resultant secondary droplets while the second provides important information to characterize the boiling morphology at the interface liquid-solid (such as bubble nucleation, bubble interactions and coalescence, or formation of local hot spots, due to non-uniform liquid vaporization).

Figure 1 depicts the temporal evolution of the boiling of HFE7100 droplets impacting with $D_0=2.0\text{mm}$ and $U_0=1.3\text{ms}^{-1}$ at different surface temperatures, T_w . Given the low effusivity ($\epsilon=(\rho k C_p)^{1/2}$) of the glass and the fact that for these surfaces the thermocouple could not be embedded in the centre of the impact region (beneath the droplet) the temperature considered here is the contact temperature, at the solid-liquid interface, as defined by Seki [19]: $T_c=(\epsilon_l T_l + \epsilon_w T_w)/(\epsilon_l + \epsilon_w)$. The contact temperature was evaluated at various wall temperatures, for both metallic and non-metallic surfaces and the trend was in agreement with the results reported by Tartarini et al. [20].

At the lower temperatures, close to the boiling temperature of the liquid $T_c=59^\circ\text{C}$, the side view of the droplets shows a regular spreading behaviour without any secondary atomization: after the kinematic phase, the lamella spreads over the surface, from the truncated sphere into a peripheral film, in an elongational flow around a stagnation region, which is also visible from the bottom view. A ring of bubbles around this region is often observed which, given the low surface temperature, cannot be attributed to thermal effects (this ring can be observed in the bottom view depicted in Figure 1a, for $t=1.0\text{ms}$). Chaves et al. [12] attribute the formation of this ring of bubbles to a rarefaction wave within the impacting droplet, which results from the reflection of the primary compression wave at the free surface of the droplet. Nucleate boiling bubbles appear later around this ring of bubbles (e.g. in Figure 1a, for $t=1.5\text{ms}$). There is no recoiling phase, but instead, the lamella spreads for very long periods, clearly dominated by capillary forces, in a behaviour which is characteristic of complete wetting systems, for small or moderate impact velocities. From the bottom views, it is clear from the image contrast that the liquid flows from the central region to the periphery, which becomes thicker as the peripheral rim is formed at later stages of the spreading. For the lower contact temperatures, wavy disturbances are observed to start at $t>4\text{ms}$ at the thin peripheral region of the lamella close to the rim, which remains weakly disturbed, and later around the stagnation region, at $t=4.5\text{ms}$. Then, a cellular structure becomes visible at the core region surrounded by the rim, as also reported by Chandra and Avedisian [21], which is attributed to surface tension gradients, due to non-uniform heat transfer during the spreading process. The cells in that structure develop in a slow process, initially increasing in number, as dry regions are formed within the lamella. At lower temperatures these cells merge and the lamella is able to keep its cohesion. However, as T_c is close or slightly

above the boiling temperature of the liquid the cell ligaments break up and the lamella is disintegrated into large liquid portions. An insipient boiling is observed for a contact temperature between 65°C and 70°C but any evident secondary atomization is visible from the side view. As the surface temperature increases, nucleation sites are observed to appear at the liquid-solid interface, associated with the emergence of small bubbles along the radial direction, which give rise to a number of waves as bubbles collapse, in a process consistent with the interpretation given by Chaves et al. [12]. The surface temperature decreases at impact and recovers slowly. There is a slow heating of the droplet by sensitive heat and when phase change occurs, even after the nucleation process has started at the liquid-surface interface, the whole process of bubble rising and further disruption of the lamella occurs quite late after the impact (only between 20~30ms after impact). However, in the vicinity of the Critical Heat Flux (CHF) condition (for T_c between 85°C and 105°C) the contact time is reduced as the lamella quickly disintegrates. The heat transfer rate is now fast enough to promote a very fast phase change, which occurs very soon after impact (between $t=1\text{ms}$ and $t=2.5\text{ms}$, in Figure 1a). Several nucleation bubbles can be observed around the ring of bubbles formed at the stagnation region and at the peripheral rim. The nucleation process occurs very fast and a very uniform distribution of bubbles can be observed within all the wetting area of the lamella (e.g. at $t=2\text{ms}$ in Figure 1a). The development of the cellular structures also occurs within a very short period of time and quickly disrupt in a violent process leading to the complete disintegration of the lamella, between $t=2.5\text{ms}$ and $t=10\text{ms}$, in Figure 1a. The rim is strongly disturbed and disrupts before $t=2.5\text{ms}$. The thermal induced atomization however occurs later, for $t>5\text{ms}$. This period corresponds to that when secondary droplets suddenly emerge at a fast rate, as previously reported, for instance in Moreira et al. [7] and in Moita and Moreira [8]. During this process, the nucleation sites leave a dry region which is no longer re-wetted as the liquid film is evaporated very fast, given the small h_{fg} of the liquid and the small thickness of the lamella. Instead, the lamella breaks up into several portions, each of them ejecting secondary droplets for a large period of time (for $t>50\text{ms}$). The most intense atomization period systematically takes place after the cell structure is complete. This process is slightly faster at the vicinity of the Critical Heat Flux condition so that, although the heat removal is larger (as it will be further shown in Figure 3), the contact area and contact period are strongly reduced as the formation of dry regions is promoted. Moreover, the surface tension, σ_{lv} , seems to play various roles in these mechanisms. Therefore, smaller surface tensions are associated to a larger spreading diameters and consequently, by mass conservation, to thinner lamellas. Hence, the whole process for the motion and collapsing of the vapour bubbles is easier and faster, so that the thermal induced atomization should begin earlier. On the other hand, the formation of cellular structures driven by surface tension gradients promote the generation of dry spots which lead to the disruption of the lamella into several portions. Therefore, the secondary atomization process should not be so violent as compared with that of a liquid with larger surface tension. Also, the Laplace pressure, responsible for the most violent bubble detachment should also be smaller for a liquid with a smaller surface tension (e.g. Mitrovic [22]) thus contributing to a less violent and finer secondary atomization process. Moreover,

considering the vapour pressure, a small h_{fg} should also contribute to a less violent secondary atomization process as the heat removal is smaller so the waiting period for the beginning of the process should be smaller. In this process, the effect of liquid viscosity cannot be neglected.

Further increasing the surface temperature, the CHF temperature is reached at the solid-liquid interface and the droplet impacts within the transition boiling regime. There is not an evident feature from bottom views within the transition boiling regime except for the very fast phase change process from the boiling, which starts as soon as the droplet contacts the surface, up to the cellular formation and complete disintegration of the lamella. Kandlikar and Steinke [13] explain the mechanisms leading to the CHF condition [13, 23] by the formation of a dryout region due to the rapid evaporation of the lamella at the liquid-solid interface, which can occur due to a nucleation cavity or near the contact line region. In this case, the vapour pressure pushes the contact line, altering the contact angle so that a thin vapour layer moves underneath the lamella. Then, depending on the force balance in the contact line region, (in which the liquid surface tension has an imperative role), and on several mechanisms such as hydrodynamic effects (e.g. Marangoni effects), adhesion forces, or the surface temperature which may not be high enough, the liquid can re-wet the surface, thus delaying the establishment of the stable film boiling regime. As this regime is established (Figure 1 b) the bottom view show disturbances in the lamella, generally occurring near the central region (e.g. at $t=2.0\text{ms}$ and $t=3.0\text{ms}$). These instabilities grow in time and become more pronounced, forming cells resembling those reported in Chaves et al. [12]. The liquid ligaments between these cells break-up, generating small secondary droplets (e.g. between $t=10\text{ms}$ and $t=18\text{ms}$). In some cases, the disturbances result in a single large cell (it is not clear here that this cell results from the coalescence of smaller cells which formed at early stages, as argued by Chaves et al. [12]), surrounded by a continuous liquid film which disintegrates as the lamella is completely disrupted from this cell. Although Chaves et al. [12] associate the formation of these cells to Rayleigh-Bernard convection, the structures observed here are more likely to be due to surface tension gradients, as those observed within the nucleate boiling regime. This may be so, since Qiao and Chandra [24] still observe these cells even at low gravity. Then, the disruption mechanism is in agreement with those reported by Chaves et al. [12]. Looking at the side images it is clear that the ejection of the secondary droplets within the radial direction occurs before the disruption of ligaments, in a process dominated by the inertial forces, which prevail over the surface tension forces. The vapour layer unbalances this competition in favour of the droplet break-up. Given these break-up mechanisms, within the film boiling regime, secondary droplet characteristics should be well correlated with both Weber and Reynolds numbers.

The morphological analysis performed up to this moment emphasizes the role of surface tension (in association with the latent heat of evaporation) in the thermal induced atomization, as suggested from the results obtained in previous work. To better infer on the main differences observed in the boiling structures and secondary atomization and their characteristic time periods, for liquids with significant dissimilar values of σ_{lv} and h_{fg} , the impact of water and HFE7100 droplets, at similar conditions, was studied in detail for various surface temperatures, again

using the two synchronized high-speed cameras. The sequence of images in Figure 2 depicts the temporal evolution of droplets impact (only bottom view is presented due to paper length constrains).

Given the low effusivity of the glass target and the higher effusivity of water, when compared to HFE7100, the contact temperature at the liquid-solid interface is significantly lower for water droplet impacts, thus requiring a larger surface heating. Moreover, the boiling temperature is significantly higher and to achieve the CHF condition also requires significantly larger superheating. Probably due to this high superheating followed by a sudden temperature decrease of the surface temperature, which is expected as the water droplet contacts the surface, because a larger amount of heat is removed at impact, it was very difficult to obtain information on the boiling morphology near the CHF condition, since the target would often break at droplet impact, damaging the coating film. In this context, different targets are being tested at the moment in order to overcome this difficulty. Due to the high h_{fg} of this liquid, a large amount of heat is removed, which is required to phase change; for a similar degree of superheat, all the boiling and further atomization process are slower. Few vapour bubbles appear only at $t>13\text{ms}$ (in Figure 2b) and the thermal induced atomization occurs only much later ($t>12\text{ms}$ after impact, within the thinner area of the lamella, around the peripheral rim. More intense boiling only occurs for $t>50\text{ms}$). Any structural cells or dry spots are visible. On the other hand, the larger surface tension precludes the disruption of the lamella and restricts the contact area, as it promotes a smaller spreading phase and an evident recoiling phase, which, in turn, contributes to thicken the liquid film which remains on the surface for quite large periods of time. Consequently for similar superheat conditions, there is a slightly larger delay between the beginning of the boiling process and that of thermal induced atomization, $[\Delta t_{(\text{beginThermIndAtom})_{\text{water}}}] \approx 15\text{ms}$; and $\Delta t_{(\text{beginThermIndAtom})_{\text{HFE7100}}} = 7\text{ms}$] as well as the time interval at which thermal induced atomization is more intense, $[\Delta t_{(\text{intenseThermIndAtom})_{\text{water}}} \approx 43.5\text{ms}$; $\Delta t_{(\text{intenseThermIndAtom})_{\text{HFE7100}}} = 20.5\text{ms}]$ (these values were obtained from the extensive image analysis, evaluating the temporal evolution of the droplet mean diameters, which was then compared to temporal evolution of the images taken from below). It is worth noting that at this stage of the work, with the transparent targets, any measurements with phase Doppler instrument or other measurement techniques were not combined yet with image analysis, so that the difference between the time intervals for both liquids may be larger, given that smaller droplets which are ejected at the beginning of the atomization are not detected in the images. Nevertheless, it is noticeable that there are differences in the boiling behaviour of the droplets of liquids with significantly different σ_{lv} and h_{fg} , which in turn will alter the secondary droplet characteristics. However, the boiling morphology becomes less different between the two liquid droplets, as they impact the surface near the CHF condition. In fact, comparing the boiling morphology at the solid-liquid interface, shown in Figure 1a) with the bottom view images reported by Kandlikar and Steinke [13], which were obtained for similar impact conditions ($D_0=2.8\text{mm}$; $U_{0\text{estimated}}$ from the data reported in [13]= 1.1ms^{-1}) near the CHF condition, it is observed that nucleate boiling starts at the lamella of the droplets of both liquids, as soon as they impact the surface ($t=1\text{ms}$ for the water droplet and $t=0.5\text{ms}$ for the HFE7100

droplet). However, the nucleate boiling occurs in a more heterogeneous distribution in the lamella of the water droplet, so that a more intense boiling occurs at the edges of the lamella, which is significantly thinner in the inner region right before the peripheral rim. This is consistent to the fact that thermal induced atomization of water droplets often starts at these regions (decreasing the delay to between the boiling mechanism and the triggering of the thermal induced atomization, at larger impact velocities, as the spreading area is larger and the lamella is thinner). A more uniform and intense boiling are only reported by Kandlikar and Steinke [13] to occur at 5ms after impact.

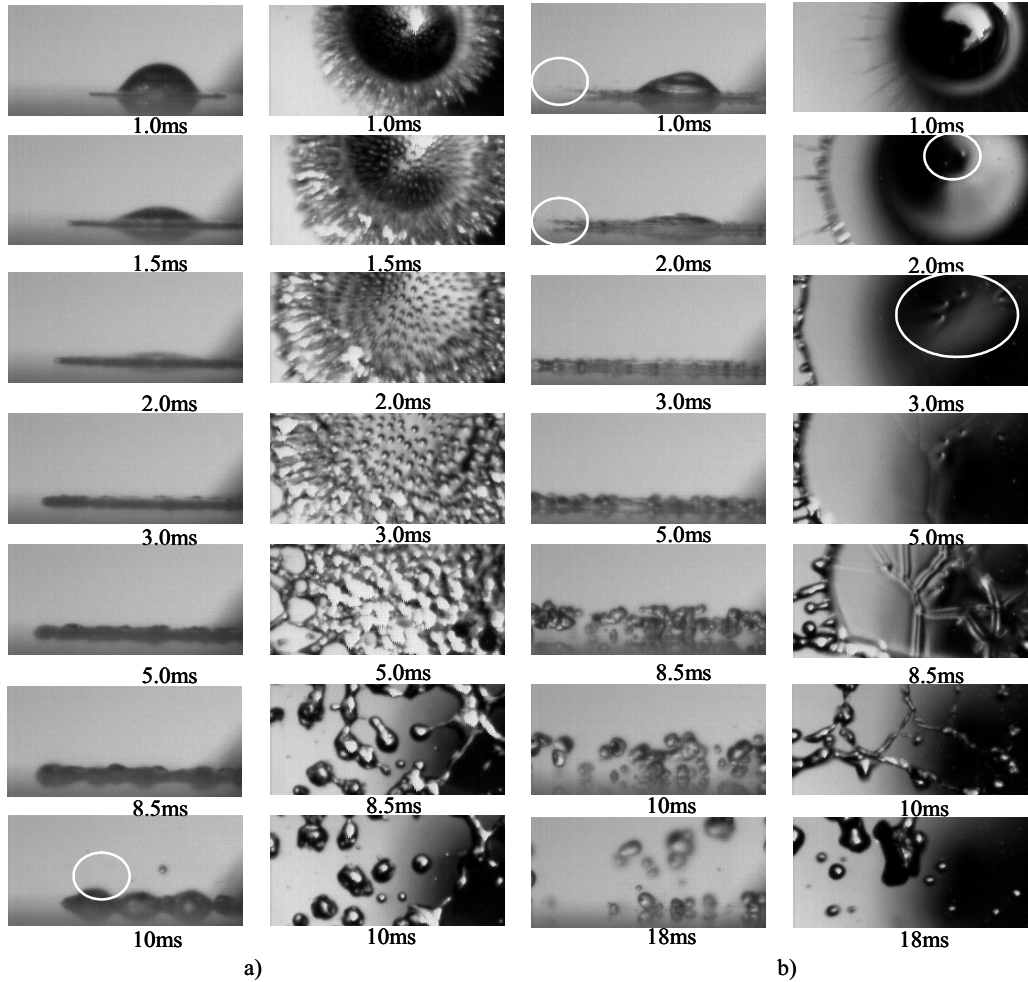


Figure 2: Details of the temporal evolution of the boiling mechanism of HFE7100 droplets ($D_0=2.0\text{mm}$, $U_0=1.3\text{ms}^{-1}$) impacting onto heated transparent substrates within different surface temperatures a) $T_c=86^\circ\text{C}$, b) $T_c=115^\circ\text{C}$.

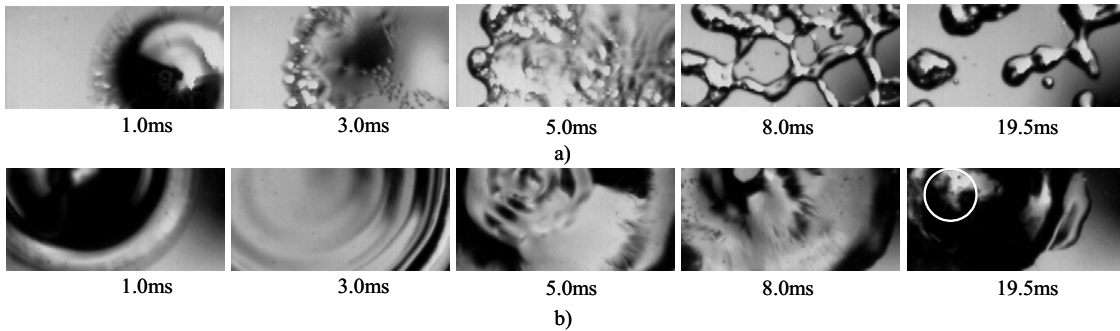


Figure 3: Details of the temporal evolution of the boiling mechanism of a) HFE7100 droplets ($D_0=2.0\text{mm}$, $U_0=1.3\text{ms}^{-1}$, $T_c=72^\circ\text{C}$); b) Water droplets ($D_0=2.0\text{mm}$, $U_0=1.3\text{ms}^{-1}$, $T_c=110^\circ\text{C}$).

On the other hand, a uniform boiling occurs very early in the HFE7100 droplet, just at $t=3\text{ms}$ after impact (Figure 1b). Furthermore, instead of the formation of a cellular mesh, with various dry spots, which promotes the fast evaporation and/or disruption of the lamella into smaller portions (as observed in the HFE7100 droplets), the bottom view sequence reported by Kandlikar and Steinke [13] shows a compact lamella within which occurs a violent and chaotic boiling.

These differences are in agreement with the abovementioned analysis concerning the role of the surface tension: the Laplace pressure, responsible for the most violent bubble detachment, is larger for a liquid with a larger surface tension. Moreover, the larger surface tension sustains the cohesion of the lamella, holding the vapour pressure. This violent boiling is also consistent with the secondary droplet characteristics, determined in previous works, which evidenced that for water, the secondary droplets are ejected with a larger momentum (e.g. Moita and Moreira [8]). An accurate relation between the characteristic times for the boiling mechanism and those for the thermal induced atomization (for instance to get more accurate correlations to describe the physical processes governing secondary droplet characteristics) requires deeper studies to obtain more detailed information, particularly on the effect of significant variations in the h_{fg} , given the experimental difficulties obtained at this point of the study. Moreover, combining other measurement techniques will provide valuable information on the velocity fields and temperature distributions in the lamella, by taking advantage on the optical access from below.

The morphological behaviour is in agreement with the temperature variation of the surface during droplet contact, referenced to the initial surface temperature. Given that the temperature variation at the impact region could not be determined for the transparent targets, these measurements were performed with targets with very high effusivity, in order to minimize this effect, which was, nevertheless, considered when establishing the initial surface temperatures to perform the experiments. Hence, for similar superheat conditions, equivalent to those considered in the morphological analysis, there is a considerable decrease in the surface temperature at droplet contacts and spreading, (first 10-20ms after impact in Figure 3), which increases with the initial surface heating, as non negligible amount of sensitive heat is removed at impact, to heat the droplet.

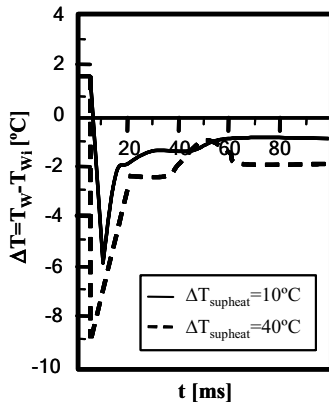


Figure 3: Surface temperature variation, measured at the point of impact of an HFE7100 droplet ($D_0=2.0\text{mm}$, $U_0=1.3\text{ms}^{-1}$) onto a smooth substrate (duralumin) within the bubble boiling regime.

Figure 4 shows that the heat removal with the water droplet is larger, as expected. The time required for the surface temperature to start recovering is also larger for the water, which should be associated not only with larger heat removal but also to the larger residence time of the lamella, which does not show cell mesh formation, generating numerous dry regions, contrarily to the HFE7100 droplet. Further increasing the surface temperature, ($T_c > 115^\circ\text{C}$), when the droplets impact within the film boiling regime, the temperature decay is quite small for the impact of HFE7100 droplets, probably due to the reduced contact between the droplet and the surface. This behaviour contrasts with that of water droplets, reported in Chen and Hsu [14] who report a strong temperature decay followed by a fast recover, at this boiling regime.

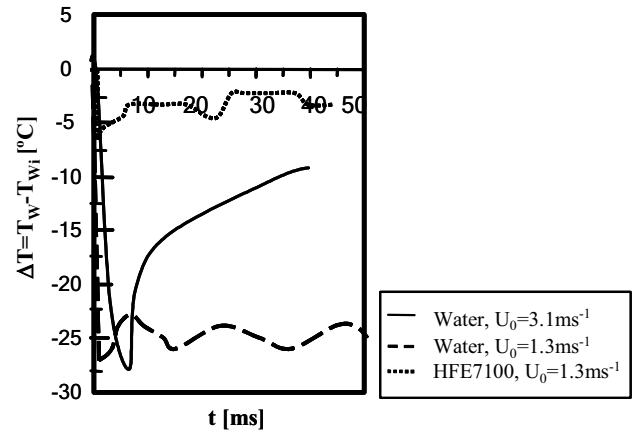


Figure 4: Surface temperature variation, measured at the point of impact of an HFE7100 droplet ($D_0=2.0\text{mm}$) and a water droplet ($D_0=2.8\text{mm}$) onto a smooth substrate (duralumin) within the bubble boiling regime ($\Delta T_{\text{supheat}}=40^\circ\text{C}$).

Increasing the impact velocity enhances the contact area and the temperature recovery is faster, in agreement with Chen and Hsu [14], but it does not provide significant additional temperature decay. Morphological differences are minor (the lamella is thinner and the spreading diameter is larger, but few differences are observed in the thermal induced atomization behaviour). Hence, the liquid properties can restrict the cooling performance, by affecting the dynamic droplet behaviour during the boiling process, for instance promoting the disruption of the lamella and generation of dry regions. The liquids with smaller surface tension and smaller h_{fg} are more likely to show these boiling characteristics which restrict their cooling performance. Under these conditions, the promoted thermal induced atomization further decreases the contact area and residence time of the lamella over the surface. These quantities can be improved by altering surface topography, as argued by several authors, but previous work (Moita and Moreira [8]) showed that the roughness parameters must be carefully chosen, in order to ensure a better performance of the system. In this context, additional experiments are being performed and, up to this moment, best performances were obtained with textured surfaces with relations of $R_a/\lambda_R=0.04$.

CONCLUSIONS

The work presented here is part of a study on the boiling morphology and boiling processes, occurring at the liquid-solid interface, of single droplets impacting onto a heated

target, to infer on their relation with thermal induced atomization mechanisms, within the various boiling regimes. For this propose, droplet impact is recorded with two synchronized high-speed cameras, positioned to obtain both side and bottom views, of the same impinging droplet. The heat transfer measurements complement the quantitative information of the system. There is a time gap between the beginning of the boiling process and the triggering of the thermal induced atomization, which depends on the liquid and on the surface properties which alter the contact area and period of the liquid over the surface. The liquid droplets with smaller surface tension and smaller latent heat of evaporation are be more likely to undergo a faster boiling process, promoting the disruption of the lamella and generation of dry regions. The thermal induced atomization further decreases the contact area and residence time of the lamella, thus degrading their cooling performance. This degradation on the cooling performance due to the dynamic behaviour of the droplet, which is altered during the boiling process can be balanced by altering the targets. These differences are less evident as one approaches the CHF condition and may be compensated by changing the surface. This boiling behaviour has consequences for the thermal induced atomization, which are in agreement with previous work. However, an accurate relation between the characteristic times for the boiling mechanism and those for the thermal induced atomization (for instance to get more accurate correlations to describe the physical processes governing secondary droplet characteristics) requires deeper studies to obtain more detailed information.

ACKNOWLEDGMENTS

The authors acknowledge the contribution of the National Foundation of Science and Technology by supporting A. S. Moita with a Fellowship (Ref:SFRH/BD/18250/2004) and by supporting the research through the project PTDC/EME-MFE/69459/2006.

NOMENCLATURE

Symbol	Quantity	SI Unit
CHF	Critical Heat Flux	W/m ²
C _p	Specific heat	KJkg ⁻¹ K
D	Initial droplet diameter	Mm
h _{fg}	Latent heat of evaporation	KJkg ⁻¹
k	Thermal conductivity	Wm ⁻¹ K ⁻¹
R _a	Mean surface roughness	μm
R _z	Average peak-to-valley surface roughness	μm
T	Temperature	°C
t	Time	Ms
U	Impact velocity (normal to the wall)	ms ⁻¹
We	Weber number	
Re	Reynolds number	
<i>Greek letters</i>		
Δt	Time interval	ms

ε	Thermal effusivity	Ws ^{1/2} m ⁻² K ⁻¹
λ	Fundamental wavelength	(μm)
ν	Kinematic viscosity	m ² s ⁻¹
θ	Equilibrium contact angle	°
ρ	Density	kgm ⁻³
σ	Surface tension	Nm ⁻¹
<i>Subscripts</i>		
0	initial	
c	contact	
l	liquid	
lv	Liquid-vapour interface	
W	Wall	

REFERENCES

- [1] P. Y. Paik, K. Chakrabarty, V. K. Pamula, Adaptive cooling of integrated circuits using digital microfluidics, *Artech House*, 2007.
- [2] E. A. Silk, J. Kim, K. Kiger, Spray cooling of enhanced surfaces: impact of structured geometry and spray axis inclination, *Int. J. H. Mass Trans.* vol. 49, pp.4910-4920, 2006.
- [3] T. A. Shedd, Next generation spray cooling: high heat flux management in compact spaces, *Heat Transfer Engineering*, Vol. 28, pp.87-92, 2007.
- [4] C. H. Amon, S.-C. Yao, C.-C. Hsieh, Microelectromechanical system-based evaporative thermal management of heat flux electronics. *Transactions of the ASME*, vol.127, 2005.
- [5] C.-C. Hsieh, S.-C. Yao, Evaporative heat transfer characteristics of a water spray on micro-structured silicon surfaces. *Int. J. Heat Mass Transf.*, vol. 49, pp. 962-974, 2006.
- [6] J. Kim, Spray cooling heat transfer: the state of the art, *Int. J. Heat Fluid Flow*, vol.28, pp.753-767, 2007.
- [7] A. L. N. Moreira, G. E. Cossali, M. Marengo, M. Santini, Secondary atomization of water and isoctane drops impinging onto tilted heated surfaces. *Exp. Fluids*, vol. 43, pp 297-313, 2007.
- [8] A. S. Moita, A. L. N. Moreira, Thermal induced atomization and heat transfer in drop impacts against surface enhanced targets, *Proceedings of the 21st Annual Conference on Liquid Atomization and Spray Systems - ILASS 2007*, Mugla, Turkey, 2007.
- [9] M. R. O. Panão and A. L. N. Moreira, Intermittent Spray Cooling: towards a new technology concept, *6th International Conference on Multiphase Flow-ICMF 2007*, Leipzig, Germany, 2007.
- [10] Tiago H. Moita, Marcelino B. dos Santos, António L. N. Moreira, Direct-Contact-Intermittent-Spray-Cooling for thermal management of a computer processor, *to be presented at the 22nd European Conference on Liquid Atomization and Spray Systems - ILASS 2008*, Como Lake, Italy, 2008.

- [11] YU A. Buyevich, B.W. Webbon, Dynamics of vapour bubbles in nucleate boiling. *Int. J. Heat Mass Transf.*, vol. 39, N° 12, pp. 2409-2426, 1996.
- [12] H. Chaves, A. M. Kubitzek, F. Obermeier, Dynamic processes occurring during the spreading of thin liquid films produced by drop impact on hot walls. *Int. J. Heat Fluid Flow*, vol. 20, pp. 470-476, 1999.
- [13] S. G. Kandlikar, Mark E. Steinke, Contact angles and interface behaviour during rapid evaporation of liquid on a heated surface. *Int. J. Heat Mass Tansf.*, vol. 45, pp. 3771-3780, 2002.
- [14] J. C. Chen, K. K. Hsu, Heat transfer during liquid contact on superheated surfaces. *J. Heat Transf.*, vol. 117, pp. 693-697, 1995.
- [15] M. Pasandideh-Fard, S. D. Aziz, S. Chandra, J. Mostaghimi, Cooling effectiveness of a water drop impinging on a hot surface. *Int. J. Heat Fluid Flow*, vol. 22, pp. 201-210, 2001.
- [16] Nunes de Carvalho, C., Lavareda, G., Parreira, P., Amaral, A. Botelho do Rego, A. M. Influence of oxygen partial pressure on the properties of undoped InO_x films deposited at room temperature by rf-PERTE, *J. Non-Crystalline Solids*, 2007, *In press*.
- [17] Silvério, V., Moreira, A. L. N. Pressure drop and heat convection in single-phase fully-developed, laminar flow in micro channels of diverse cross section, 5th *European Thermal-Science Conference*, Eindhoven University of Technology, The Netherlands, 2008.
- [18] A. S. Moita, A. L. N. Moreira. Drop impacts onto cold and heated rigid surfaces: morphological comparisons, disintegration limits and secondary atomization. *Int. J. Heat Fluid Flow*, vol. 28, N°4, pp.735-752, 2007.
- [19] M. Seki, H. Kawamura, K. Sanokawa, Transient temperature profile of a hot wall due to an impinging liquid droplet. *ASME J. Heat Transf.*, vol. 100, pp. 167-169, 1978.
- [20] P. Tartarini, G. Lorenzini, M. R. Randi, Experimental study of water droplet boiling on hot, non porous surfaces. *Heat Mass Transf.*, vol. 34, pp. 437-447, 1999.
- [21] S. Chandra, C. T. Avedisian, On the collision of a droplet with a solid surface. *Proc. R. Soc. London, Ser.A*, vol. 432, pp. 13-41, 1991.
- [22] J. Mitrovic, Formation of a liquid jet after detachment of a vapour bubble. *Int. J. Heat Mass Transf.*, vol. 40, N° 18, pp. 4309-4317, 1997.
- [23] S. G. Kandlikar, A theoretical model to predict pool boiling CHF incorporating effects of contact angle and orientation. Paper presented in the session on Fundamentals of Critical Heat Flux in Pool and Flow Boiling, in: *ASME National Heat Transfer Conference*, Pittsburgh, 2000, *ASME J. Heat Transfer*, vol. 123, pp. 1071-1079, 2001.
- [24] Y.M. Qiao, S. Chandra, Boiling of droplets on a hot surface in low gravity. *Int. J. Heat Mass Transf.*, vol. 39, pp. 1379-1393, 1996.